Contribution from the Department of Chemistry,
University of Tennessee, Knoxville, Tennessee 37916

Electrochemistry of Zirconium(IV) in Chloroaluminate Melts

BERNARD GILBERT, GLEB MAMANTOV,*[1] and K. W. FUNG

Received December 9, 1974 AIC40820Z

The electrochemical reduction of zirconium(IV), added as either $ZrCl_4$ or Na_2ZrCl_6, in molten $AlCl_3$–NaCl (51–52 mol % $AlCl_3$) at 175–220°, results in the formation of insoluble $ZrCl_3$. The Raman spectrum of $ZrCl_3$ is reported. The reduction process involves nucleation overpotential as indicated by the maxima in chronoamperometric current–time curves, potential overshoots in chronopotentiograms, and a large anodic shift of the peak potential of the reduction process in subsequent cyclic voltammetric scans (provided $ZrCl_3$ deposit is not completely removed). The complete oxidation of the $ZrCl_3$ deposit in cyclic voltammetry experiments at low scan rates (<0.1 V/sec) occurs at potentials which are nearly 1 V more anodic than the peak potential for the corresponding reduction process. The complete oxidation of $ZrCl_3$ appears to be controlled by the availability of Cl^- ions. The diffusion coefficients of Zr(IV) in this medium at several temperatures are reported. The reduction of Zr(IV) in very acidic chloroaluminate melts, for example, $AlCl_3$–NaCl (60 mol % $AlCl_3$), results in the formation of Zr(II) at high temperatures (>250°) and of soluble Zr(III) at low temperatures (<140°), which apparently disproportionates to Zr(IV) and Zr(II).

Introduction

The coordination and redox chemistry of various elements in chloroaluminate ($AlCl_3$–MCl mixtures where M^+ is an alkali cation) melts has been the subject of several recent investigations.[2] The molten chloroaluminates have indeed been shown to be interesting solvents for studying coordination equilibria[3,4] and electrochemical[5] and spectral studies.[6–11] They can be characterized by low liquidus temperatures, relatively high decomposition potentials, and a wide range of optical transparency. The Lewis acidity can be varied widely by changing the $AlCl_3$–MCl ratio. In acidic mixtures unusually low oxidation states of several elements have been obtained; the disproportionation of these states is a function of the acidity of the melt.[7,9,12,13] We have recently initiated a systematic study of the electrochemistry and chemistry of elements in groups 4B–6B in chloroaluminate melts. This work, dealing with the electrochemistry of zirconium, follows our previous investigation of the Ti(II) behavior in chloroaluminates.[14]

The electrochemistry of zirconium tetrachloride in molten salts has been studied mainly in molten alkali halide mixtures. In these solvents, the $ZrCl_4$ reduction is to a great extent determined by temperature;[15–19] at low temperatures (below 400°) one observes simply $Zr^{4+} + 4e^- \rightleftarrows Zr$; at temperatures above 500°, the reduction occurs in two steps: $Zr^{4+} + 2e^- \rightleftarrows Zr^{2+}$ and $Zr^{2+} + 2e^- \rightleftarrows Zr$. However, this mechanism is probably more complex because several authors have evidence for the existence of Zr^{3+}. For example, Flengas and Swaroop[20] proposed that $ZrCl_3$ is stable in NaCl–KCl melts and that the reduction of Zr^{4+} between 670 and 740° involves three steps: $Zr^{4+} \rightleftarrows Zr^{3+} \rightleftarrows Zr^{2+} \rightleftarrows Zr$. Similarly, the electrochemical formation of Zr^{3+} has apparently been observed in the chronopotentiometric investigations of Sakakura.[21]

Larsen et al.[22] have recently used pure molten Al_2Cl_6 as the solvent for the preparation of $ZrCl_3$ by the reduction of $ZrCl_4$ with zirconium or aluminum metal. In the presence of $ZrCl_4$, an incompletely characterized soluble blue Zr(III) compound is formed before the deposition of the green $ZrCl_3$ crystals. $ZrCl_3$ is unstable in pure Al_2Cl_6; a brown product $2(ZrCl_2)\cdot AlCl_3$ is obtained. Chloroaluminates have also been used as solvents for the purification of $ZrCl_4$ involving a reduction step by an active metal or $ZrCl_2$.[23]

In the present investigation, we have attempted to characterize electrochemically the reduction products of Zr^{4+} in several molten $AlCl_3$–NaCl mixtures.

Experimental Section

$ZrCl_4$ (Reactor grade, Alfa Products) was purified by the reaction with copper at 160° to remove oxide impurities[24] and then sublimed several times until the final product was completely white. Na_2ZrCl_6 was synthesized by a solid–gas reaction between $ZrCl_4$ and NaCl as described by Lister and Flengas.[24] The procedure for preparing acidic ($AlCl_3$ content higher than 50 mol %) mixtures has been described previously.[13,25] Recrystallized, dry NaCl was mixed with sublimed $AlCl_3$ ("Iron Free" from Fluka) and aluminum metal (m5N from Alfa Products) and the mixture was digested for several days at 300°. In the case of basic melts ($AlCl_3$ content less than 50 mol %) it was preferable to electrolyze the molten mixture using a pair of aluminum electrodes as described by Boxall et al.[26] Handling and preparation of the mixture were done in an argon-filled Vacuum Atmospheres Model HE 43-2 drybox equipped with a Model HE-493 Dri-Train capable of oxygen and moisture removal to <1 ppm. The electrochemical cell, furnace, and procedure have been previously described[13,25] except that the temperature stability of the furnace has been improved by using a better insulation and a homemade temperature controller. The electrodes used in this study were made of platinum, tungsten, or glassy carbon. Because of the high resistance of the Pyrex membrane of the reference compartment, a platinum quasireference electrode was used in cyclic voltammetric, polarographic, and chronopotentiometric measurements. The potential of this electrode with respect to the aluminum reference electrode was monitored continuously with a Keithley electrometer. For measurements involving coulometry, the reference aluminum electrode and the platinum counter electrode were separated from the bulk solution by either a Pyrex or a Radiometer[11] frit.

Voltammograms, chronopotentiograms, and current–time curves were obtained with a controlled-potential cyclic voltammeter.[27] Polarograms were also obtained with a PAR Model 174 pulse polarograph using normal or differential modes. Coulometric experiments were performed with a Wenking potentiostat, Model 66TS3. The curves were recorded with a Moseley 2D-2A X-Y recorder or a Type 549 Tektronix storage oscilloscope with a Polaroid camera.

The chemical analysis of the precipitate (see below) was performed as follows. Zirconium and aluminum were determined by atomic absorption at the Oak Ridge National Laboratory and by EDTA titrations.[28] The chlorine and sodium contents were obtained by potentiometric or Volhard titrations and flame emission spectroscopy, respectively. The nature of the precipitate was confirmed by comparing its X-ray powder pattern with the previously published patterns.

A Cary 81 monochromator coupled with a cooled 9658 EMI photomultiplier and a photon counting system was used to record the Raman spectrum of the precipitate. The exciting line was the 632.8-nm line of a Model 125 He–Ne laser. By using the 488.0- or 514.5-nm line of an argon ion laser, one obtains very poor spectra and the sample is decomposed. The sample was contained in a small evacuated Pyrex tube which was placed in the path of the laser beam. The details of the procedure have been described before.[13]

Results and Discussion

Zr(IV) was added to the melt as $ZrCl_4$ or Na_2ZrCl_6. The results obtained were independent of the nature of the starting material; thus, $ZrCl_4$ and Na_2ZrCl_6 are probably present in

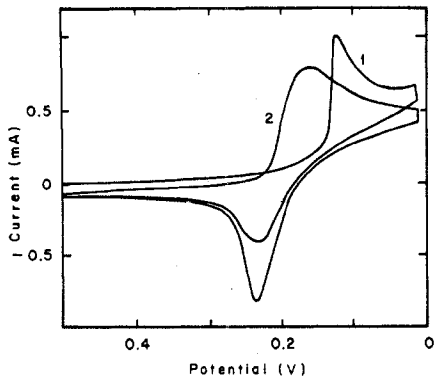

Figure 1. Cyclic voltammogram for Zr^{4+} at a platinum electrode in $AlCl_3$-NaCl (52 mol % $AlCl_3$). $T = 175°$; $v = 0.1$ V sec^{-1}; Zr^{4+} concentration is 5×10^{-2} M; the numbers 1 and 2 refer to the first and second cycle, respectively; electrode area = ≃0.1 cm^2.

Table I. Variation of i_p/C vs. C

10^2C, M		i_p/C, A M^{-1}		
175°	218°	175°	218°	Electrode
4.38	4.28	2.13	2.94	Platinum
3.43	3.35	2.12	2.98	
2.58	2.52	2.23	2.98	
1.41	1.38	2.13	2.93	
4.38	4.28	3.45	4.79	Tungsten
3.43	3.35	3.42	4.78	
2.58	2.52	3.48	4.76	
1.41	1.38	3.54	4.89	

the same form in the melt. Both are soluble in acidic melts and in the $AlCl_3$–NaCl (50 mol % $AlCl_3$) melt until a concentration of about 8×10^{-2} M at 200° is reached. The dissolution is, however, extremely slow. In the NaCl-saturated melt $ZrCl_4$ and Na_2ZrCl_6 are insoluble and the waves obtained by cyclic voltammetry in acidic mixtures disappear when an excess of NaCl is added to an acidic melt. Because of the solubility problem and because of the fact that it is very difficult to prepare an exact 50:50 mol % mixture, the composition of our melts was varied from 63 to 51 mol % $AlCl_3$. The experimental results were found to be very sensitive to the composition of the melt. The electrochemical behavior of Zr(IV) will be described first for a composition close to 50 mol % and second for a melt of 60 mol % $AlCl_3$.

A. Electrochemical Behavior in $AlCl_3$–NaCl (51–52 mol % $AlCl_3$) Mixtures. 1. Cyclic Voltammetry. A typical voltammetric wave obtained with a solution of $ZrCl_4$ in the melt which is 52 mol % $AlCl_3$ is given in Figure 1. The potentials are referred to the potential of an aluminum electrode in a melt of the same composition. To convert to a 63 or a 50 mol % $AlCl_3$ reference compartment composition, appropriate potentials have to be added.[29] A very well-defined reduction–oxidation wave is observed close to the reduction of aluminum. The peak potential of the reduction wave is about 120 mV before the reduction of aluminum. However, for the second cycle, the reduction wave is shifted with respect to the first cycle by about +60 to +80 mV. If the electrode is then held at its initial potential (+0.5 V) for 10 min and the scan is started again, the wave corresponds to the first cycle. To understand this phenomenon, the following points were considered.

Characteristics of the Reduction Wave Corresponding to the First Cycle. (1) A sharp increase in current at the beginning of the wave is characteristic of the deposition of an insoluble product.[30] (2) The peak current (i_p) is proportional to the concentration of $ZrCl_4$ at both Pt and W electrodes at the two temperatures investigated (175 and 218°) (Table I). (3) If the scan rate is varied, the following facts are observed. (a) The peak current is proportional to $v^{1/2}$ (v = scan rate) in the range of 0.01–5 V sec^{-1} at both Pt and W electrodes. This result indicates a lack of chemical complications.[31] (b) If the reduction cycles are repeated, the second-cycle reduction wave is removed (60 mV) from the first-cycle wave at low scan rates (0.1 V sec^{-1}); it moves closer to the first-cycle wave if the scan rate is increased. Above a scan rate of 2 V sec^{-1}, only one reduction wave corresponding to the potential of the first cycle is obtained even after several cycles.

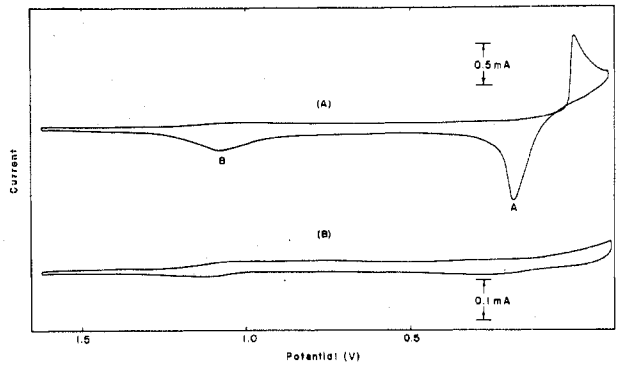

Figure 2. Cyclic voltammogram for Zr^{4+}. Melt composition is $AlCl_3$-NaCl (51 mol % $AlCl_3$); Zr^{4+} concentration is 3.35×10^{-2} M; $T = 218°$; Pt electrode area is 0.086 cm^2; scan rate is 0.1 V sec^{-1}; for waves A and B, see text. Curve B corresponds to the background at the same electrode in the absence of Zr^{4+}.

Reoxidation of the Deposit. During the oxidation of the deposit, one observes in addition to a well-defined oxidation wave (wave A) at about +0.23 V before the aluminum deposition a second wave (B) (Figure 2). This second wave is very broad; its intensity and position are not very reproducible but depend on the temperature, the concentration, and the scan rate.

(1) Characteristics of Wave A. Its position is independent of the scan rate. The ratio $(i_p)_a/(i_p)_c$[31] increases with the scan rate and becomes constant above 2 V sec^{-1}. At low scan rates, $(i_p)_a/(i_p)_c$ increases with the temperature.

(2) Characteristics of Wave B. At low scan rates (<0.1 V sec^{-1}), wave B is located at potentials greater than 1 V from the reduction of aluminum. It is, thus, clear that the potential range in Figure 1 is not large enough to oxidize the deposit. The nature of the electrode surface changes between the beginning and the end of the first cycle and the anodic shift of the reduction wave for the second cycle is apparently due to a change in the nucleation overpotential (see below). Indeed, if the scanned potential range is extended to 1.5 V and the other experimental conditions of Figure 1 are maintained, the deposit is completely oxidized and one obtains even after several successive cycles only the reduction wave corresponding to the first cycle. Furthermore, when the scan rate is increased, wave B becomes smaller and shifts toward wave A. At about 2 V sec^{-1} and higher scan rates, both waves coincide; there is consequently no difference between the first- and the second-cycle waves.

The presence of two oxidation waves and their behavior with respect to the scan rate, the concentration, the temperature, and the acidity of the melt are similar to that observed in the case of Fe^{2+} in chloroaluminate melts.[26] However, the separation between the two oxidation waves is much greater in the case of zirconium; a shift of the second oxidation wave with the scan rate was not reported for Fe^{2+}. A somewhat different explanation is proposed for Zr(IV). Since it will be shown below that the oxidation state of the deposit is +3 and that the solid corresponds to $ZrCl_3$, waves A and B are believed to involve the oxidation of $ZrCl_3$ to $ZrCl_4$. Wave A corresponds to the beginning of the oxidation of the deposit; readily available Cl^- ions are consumed. If the production of Zr(IV) increases (a higher concentration of the starting material or

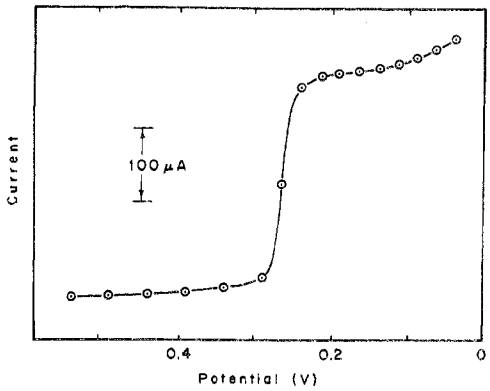

Figure 3. Polarograms constructed from current-time curves at a platinum electrode (area ≃0.1 cm²). Na_2ZrCl_6 concentration 3 × 10^{-2} *M*; *T* = 197°; current was measured at 2.5 sec; melt composition is $AlCl_3$–NaCl (50.5 mol % $AlCl_3$).

a lower scan rate), the amount of Cl^- in the immediate vicinity of the electrode is not high enough to complete the oxidation of the deposit. The oxidation of the remaining deposit (wave B) is then apparently limited by the supply of Cl^- ions which are brought by diffusion or by reactions such as $2AlCl_4^- \rightarrow Al_2Cl_7^- + Cl^-$. The position and the intensity of wave B will then depend on the availability of Cl^- ions at the electrode surface and consequently on the acidity of the melt, on the temperature (which influences the diffusion rate), and on the time between two successive scans as it was observed. The $ZrCl_4$ produced on reoxidation is thus very probably solvated as proposed by Larsen et al.[22]

2. Determination of the Oxidation State of the Reduced Form. Several experiments were performed in order to evaluate the number of electrons corresponding to the reduction wave. Polarograms were constructed from current–time curves;[13] a typical example is shown in Figure 3. The diffusion plateau is well defined; the diffusion current is proportional to the $ZrCl_4$ concentration up to 5 × 10^{-2} *M*. The pulse polarographic diffusion current is also proportional to concentration in the same concentration range. However, current–time curves exhibit an anomalous behavior in a certain potential range. The shape of the *i*–*t* curve is normal ($it^{1/2}$ is constant)[32] for applied potentials corresponding to the plateau. At potentials close to $E_{1/2}$, the curves show a maximum; position and the intensity of this maximum depend greatly on the applied potential (Figure 4). The polarograms constructed from these *i*–*t* curves are strongly distorted exhibiting a sudden increase in current for a very small change of potential in the range of $E_{1/2}$.

A maximum in the *i*–*t* curves can be explained as resulting from an ECE (ECE is a frequently used notation for the scheme involving electrochemical, chemical, and electrochemical steps in sequence) mechanism[33] or arising from a reduction controlled by the nucleation rate in the initial step of the deposit formation. The latter behavior has been observed recently for the deposition of palladium in aqueous solutions.[34] The chronoamperometric and voltammetric curves obtained in this case are similar to those that we observed. We also observed similar *i*–*t* curves for the reduction of Fe^{2+} in molten $NaAlCl_4$; this system has been studied previously[26] and does not involve an ECE mechanism. The chronopotentiograms for the Zr(IV) reduction were distorted by an overshoot at the beginning of the wave; this overshoot is similar to the one observed by Stromatt[35] and by Martinot and Duyckaerts[36] for the deposition of an insoluble product and corresponds to a nucleation peak. Thus, the reduction of Zr^{4+} and Fe^{2+} involves a slow nucleation at the beginning of the wave; no information on the number of electrons can be obtained from the slope of the polarograms or chronopotentiograms. The number of

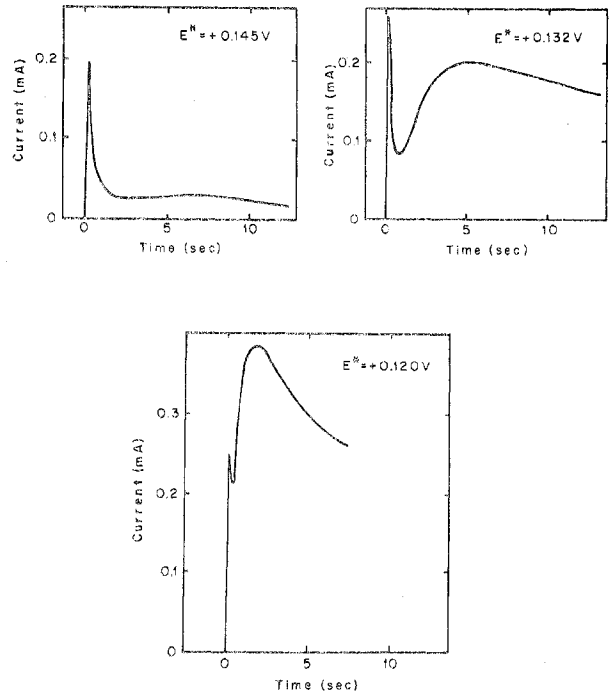

Figure 4. Current–time curves obtained by applying three different potentials in the vicinity of $E_{1/2}$. Melt composition is $AlCl_3$–NaCl (51 mol % $AlCl_3$); Zr^{4+} concentration is 4.28 × 10^{-2} *M*; *T* = 218°; *E** is the potential applied to a W electrode with respect to an Al reference electrode in $AlCl_3$–NaCl (51 mol % $AlCl_3$). The initial potential was set at 1.5 V after every run.

Table II. Calculated Values of "*n*" from $(i_p/v^{1/2})/it^{1/2}$ Ratios

Temp, °C	Electrode	$10^2 C_{ZrCl_4}$, *M*	Calcd *n*
222	Platinum	2.80	0.99
200	Tungsten	1.39	1.1[a]
			1.02[b]
200	Platinum	1.39	1.02[a]
			0.90[b]

[a] Calculated from the measurements with the X-Y recorder. [b] Calculated from the measurements at shorter times with the oscilloscope.

electrons can, however, be calculated when the current is controlled by diffusion. By relating the voltammetric $i_p/v^{1/2}$ and chronoamperometric $it^{1/2}$ for an insoluble product[30,32] (providing that the current–time curve is obtained at a potential corresponding to the diffusion plateau of the polarogram) one obtains

$$n^{1/2} = \frac{R^{1/2}T^{1/2}i_p}{0.610\pi^{1/2}F^{1/2}v^{1/2}it^{1/2}}$$

Examples of "*n*" values calculated by this method are given in Table II.

For the case of an insoluble product, the peak potential of the voltammetric wave should shift in an anodic direction with an increase of concentration as may be seen from the equation[30]

$$E_p = E^\circ + \frac{RT}{nF}\ln fC - 0.854\frac{RT}{nF}$$

Linear plots of E_p vs. log *C* were obtained. The theoretical slopes for a one-electron process (assuming that the activity coefficient *f* remains constant) at 218 and 175° are 0.0975 and 0.088 V, respectively. The corresponding measured slopes were 0.103 and 0.077 V. The respective values of E° are +0.275 and +0.250 V (assuming *f* = 1) with respect to an Al electrode in a melt of the same composition.

To confirm a value of *n* = 1, we have also performed a controlled-potential coulometric reduction of Zr^{4+} in the melt.

Table III. Calculated Diffusion Coefficients

Temp, °C	Electrode	$10^2C, M$	Method	10^6D, $cm^2\ sec^{-1}$
200	Platinum	1.39	$i_p/v^{1/2}$	9.4
200	Tungsten	1.39	$i_p/v^{1/2}$	9.4
200	Platinum	1.39	$it^{1/2}$	10.7[a]
				9.4[b]
200	Tungsten	1.39	$it^{1/2}$	9.4[a]
				8.6[b]
175	Platinum		i_p vs. C	7.0
175	Tungsten		i_p vs. C	7.2
218	Platinum		i_p vs. C	14.0
218	Tungsten		i_p vs. C	14.4

[a] Footnote *a* of Table II. [b] Footnote *b* of Table II.

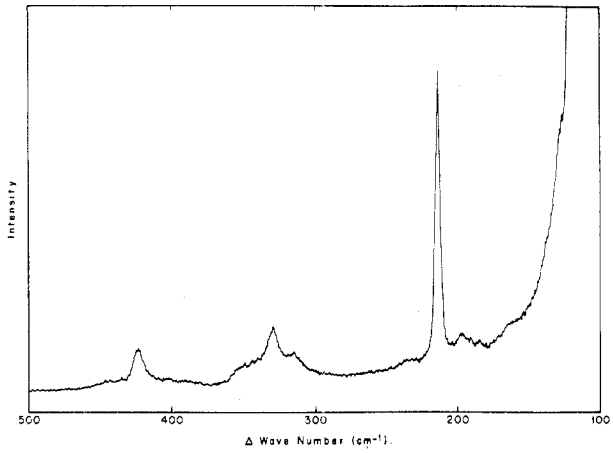

Figure 5. Raman spectrum of solid $ZrCl_3$. Exciting line is 632.8 nm (20 mW); slit width is 4 cm^{-1}; RC = 0.5 sec.

The method and the experimental set up were first checked for the oxidation of Ti^{2+} in acidic chloroaluminates.[14] In the case of Zr^{4+}, the slope of the linear log i vs. time plot for two different concentrations gave $n = 0.92$ and 0.94. The reduction step is then

$$Zr^{4+} + e^- \rightleftarrows Zr^{3+}$$

Knowing the value of n, the diffusion coefficients have been calculated; the experimental results are summarized in Table III. The surface area of the platinum electrode was determined from current–time curves obtained with a 5×10^{-3} M aqueous solution of $Fe(CN)_6^{3-}$ in 1 M KCl.[37] For the same aqueous conditions, the results were not reproducible for the tungsten electrode; its surface area was calculated from the average ratio of currents obtained at W and Pt electrodes in the molten salt experiments.

3. Nature of the Deposit. At the end of the coulometric experiment, dark green-yellow crystals were found on the bottom of the cell. The crystals are identical in color with $ZrCl_3$ prepared in liquid $AlCl_3$ by Larsen et al.[22] The formation of black $ZrCl_2$ is apparently excluded. After filtration of the crystals, an X-ray powder pattern was obtained and found to be essentially the same as the one published by Watts[38] and by Dahl et al.[39] for $ZrCl_3$. The difference is due to a small contamination by $NaAlCl_4$ which was also found by chemical analysis. In view of this contamination by the melt (somewhat variable from one experiment to another), the analytical data for $ZrCl_3$ were only useful to confirm the results obtained from X-ray powder patterns.

To our knowledge, the Raman spectrum of $ZrCl_3$ has not yet been published. It is shown in Figure 5. The special feature of this spectrum is the very strong and sharp line at 212 cm^{-1} which is probably due to a metal–metal bond. Dahl et al.[39] have shown by a simple molecular orbital treatment that metal–metal bonds are feasible in the proposed structure which consists of a hexagonal lattice containing linear polymer chains of octahedral $ZrCl_6$ units.[38] The next most intense band in the spectrum falls at 329 cm^{-1}; from a comparison with Cs_2ZrCl_6 spectra,[40] it probably corresponds to the ZrCl vibration of the $ZrCl_6$ unit.

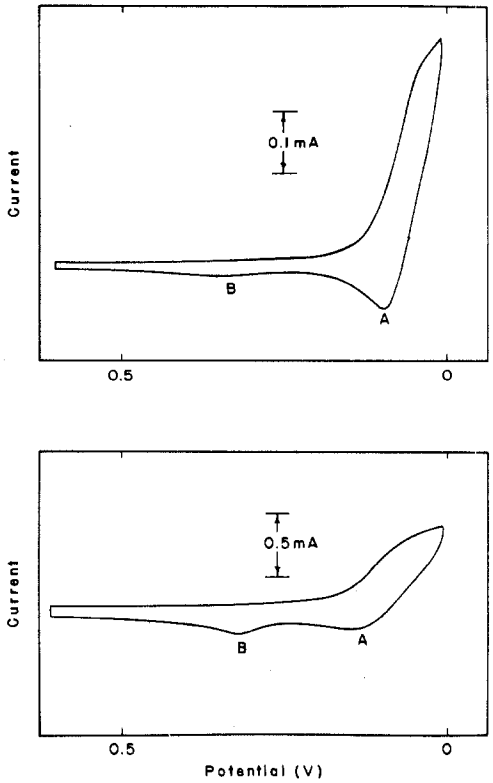

Figure 6. Cyclic voltammograms for Zr^{4+} in $AlCl_3$–NaCl (60 mol % $AlCl_3$) at a platinum electrode (area 0.086 cm^2). Upper curve: $T = 269°$; $[Zr^{4+}] = 4.2 \times 10^{-2}$ M; scan rate 0.005 V sec^{-1}. Lower curve: $T = 175°$; $[Zr^{4+}] = 4.38 \times 10^{-2}$ M; scan rate 0.05 V sec^{-1}.

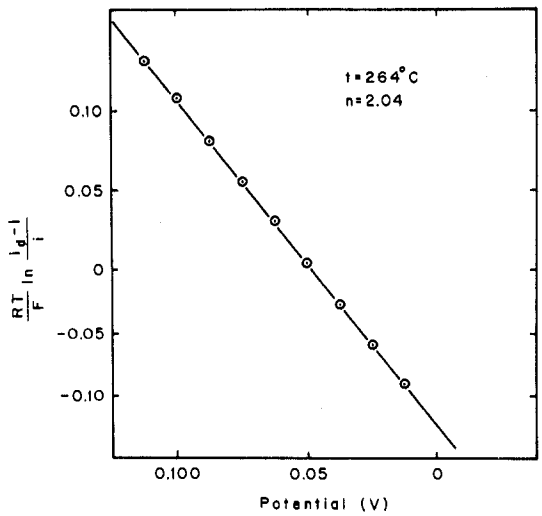

Figure 7. log $[(i_d - i)/i]$ vs. E plot at a W electrode (0.136 cm^2). Melt composition is $AlCl_3$–NaCl (60 mol % $AlCl_3$); $T = 264°$; $[Zr^{4+}] = 4.2 \times 10^{-2}$ M.

B. Behavior in $AlCl_3$–NaCl (60–40 mol %) Melt. In very acidic mixtures, one reduction wave and two oxidation waves are observed but their characteristics and behavior are very different from those obtained for the melts studied in the previous section. Examples of cyclic voltammograms in $AlCl_3$–NaCl (60 mol % $AlCl_3$) are shown in Figure 6. The reduction wave occurs very close to the aluminum reduction and consequently is not well defined. It was not possible to make accurate measurements of peak currents or peak potentials. The main difference compared to the results obtained

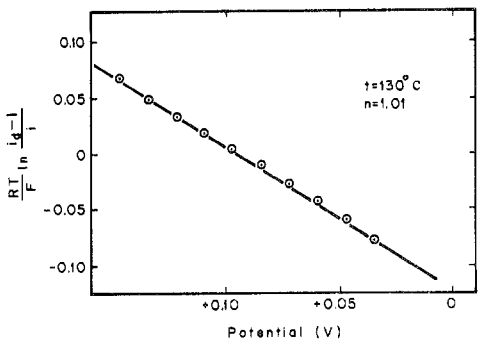

Figure 8. log $[(i_d - i)/i]$ vs. E plot at a W electrode (0.136 cm^2). Melt composition is $AlCl_3$-NaCl (60 mol % $AlCl_3$); $T = 130°$; $[Zr^{4+}] = 4.45 \times 10^{-2}$ M.

in the previous section is that the reduction wave corresponds in this case to the formation of a soluble product. Chronoamperometric curves did not exhibit maxima.

The results were found to be very dependent on the temperature and the scan rate. The slopes of the polarograms constructed from current–time curves change markedly with temperature. At high temperatures (above 250°), n calculated from the linear plot log $[(i_d - i)/i]$ vs. E (in which i_d is measured by the extrapolation of the polarographic wave) is equal to 2 (Figure 7). At low temperatures (below 140°) the same plot gives $n \simeq 1$ (Figure 8).

The first oxidation wave (wave A in Figure 6) predominates at high temperatures and low scan rates; the second oxidation wave (wave B in Figure 6) prevails at low temperatures. A mechanism involving the reduction of Zr^{4+} to Zr^{3+} followed by a disproportionation of Zr^{3+} into Zr^{4+} and Zr^{2+} (slow at low temperatures but fast at high temperatures) is consistent with the experimental results. Such a disproportionation was also proposed in very acidic melts by Larsen et al.[22] to explain the limited efficiency in producing $ZrCl_3$ and the appearance of a lower oxidation state product. Due to the proximity of the Al reduction, it was not possible to perform the necessary quantitative measurements in order to confirm this mechanism.

Acknowledgment. This research was supported by the National Science Foundation under Grants GP 32433X and 43405X. We wish to thank G. M. Begun of Oak Ridge National Laboratory for the use of his Raman spectrometer and J. H. Burns of Oak Ridge National Laboratory for the help with the X-ray powder diffraction work.

Registry No. Zr(IV), 15543-40-5; $ZrCl_4$, 10026-11-6; Na_2ZrCl_6, 18346-98-0; $ZrCl_3$, 10241-03-9.

References and Notes

(1) To whom correspondence should be addressed.
(2) For a review, see C. R. Boston, *Adv. Molten Salt Chem.*, **1**, 129–163 (1971).
(3) H. A. Oye, *Acta Chem. Scand.*, **26**, 1640 (1972).
(4) T. Kvaal and H. A. Oye, *Acta Chem. Scand.*, **26**, 1647 (1972).
(5) For a brief review see K. W. Fung and G. Mamantov, *Adv. Molten Salt Chem.*, **2**, 218–224 (1973).
(6) J. Brynestad and G. P. Smith, *J. Am. Chem. Soc.*, **92**, 3198 (1970).
(7) N. J. Bjerrum and G. P. Smith, *J. Am. Chem. Soc.*, **90**, 4472 (1968).
(8) N. J. Bjerrum, C. R. Boston, and G. P. Smith, *Inorg. Chem.*, **6**, 1162 (1967).
(9) N. J. Bjerrum, *Inorg. Chem.*, **9**, 1965 (1970); **10**, 2578 (1971); **11**, 2648 (1972).
(10) J. H. von Barner and N. J. Bjerrum, *Inorg. Chem.*, **12**, 1891 (1973).
(11) J. H. von Barner, N. J. Bjerrum, and K. Kiens, *Inorg. Chem.*, **13**, 1708 (1974).
(12) T. C. F. Munday and J. D. Corbett, *Inorg. Chem.*, **5**, 1263 (1966).
(13) G. Torsi, K. W. Fung, G. M. Begun, and G. Mamantov, *Inorg. Chem.*, **10**, 2285 (1971).
(14) K. W. Fung and G. Mamantov, *J. Electroanal. Chem.*, **35**, 27 (1972).
(15) C. Eon, C. Pommier, J. C. Fondanaiche, and H. Fould, *Bull. Soc. Chim. Fr.*, 2574 (1969).
(16) R. Baboian, D. L. Hill, and R. A. Bailey, *J. Electrochem. Soc.*, **112**, 1221 (1965).
(17) V. T. Barchuk and I. N. Sheiko, *Sov. Prog. Chem. (Engl. Transl.)*, **33**, 18 (1967).
(18) T. Suzuki, *Denki Kagaku Oyobi Kogyo Butsuri Kagaku*, **39**, 864 (1971).
(19) M. V. Smirnov, A. N. Baraboshkin, and V. E. Komarov, *Russ. J. Phys. Chem. (Engl Transl.)*, **37**, 901 (1963).
(20) B. Swaroop and S. N. Flengas, *Can. J. Chem.*, **44**, 199 (1966).
(21) T. Sakakura, *J. Electrochem. Soc. Jpn.*, **35**, 75 (1967).
(22) E. M. Larsen, F. Gil-Arnao, J. W. Moyer, and M. J. Camp, *Chem. Commun.*, 281 (1970); *Inorg. Chem.*, **13**, 574 (1974).
(23) I. E. Newnham, U.S. Patent 2,916,350 (Dec 8, 1959); *Chem. Abstr.*, **54**, 13579 (1960).
(24) R. L. Lister and S. N. Flengas, *Can. J. Chem.*, **42**, 1102 (1964).
(25) G. Torsi and G. Mamantov, *J. Electroanal. Chem.*, **30**, 193 (1971).
(26) L. G. Boxall, H. L. Jones, and R. A. Osteryoung, *J. Electrochem. Soc.*, **121**, 212 (1974).
(27) T. R. Mueller and H. C. Jones, *Chem. Instrum.*, **2**, 65 (1969).
(28) G. Schwarzenbach, "Complexometric Titrations", Interscience, New York, N.Y., 1957.
(29) L. G. Boxall, H. L. Jones, and R. A. Osteryoung, *J. Electrochem. Soc.*, **120**, 223 (1973).
(30) P. Delahay "New Instrumental Methods in Electrochemistry", Interscience, New York, N.Y., 1954, p 122.
(31) R. S. Nicholson and I. Shain, *Anal. Chem.*, **36**, 706 (1964).
(32) P. Delahay, "New Instrumental Methods in Electrochemistry", Interscience, New York, N.Y., 1954, p 51.
(33) R. Buchta and D. H. Evans, *Anal. Chem.*, **40**, 2181 (1968).
(34) M. F. Bell and J. A. Harrison, *J. Electroanal. Chem.*, **41**, 15 (1973).
(35) R. W. Stromatt, *J. Electrochem. Soc.*, **110**, 1277 (1963).
(36) L. Martinot and G. Duyckaerts, *Inorg. Nucl. Chem. Lett.*, **5**, 909 (1969).
(37) R. N. Adams, "Electrochemistry at Solid Electrodes", Marcel Dekker, New York, N.Y., 1969.
(38) J. A. Watts, *Inorg. Chem.*, **5**, 281 (1966).
(39) L. F. Dahl, T. I. Chiang, P. W. Seabaugh, and E. M. Larsen, *Inorg. Chem.*, **3**, 1236 (1964).
(40) W. van Bronswyk, R. J. H. Clark, and L. Maresca, *Inorg. Chem.*, **8**, 1395 (1969).